Classical and quantal atomic form factors for $nlm \rightarrow n'l'm$ transitions

M. R. Flannery and D. Vrinceanu
School of Physics, Georgia Institute of Technology, Atlanta, Georgia 30332-0430
(Received 17 July 2001; published 4 January 2002)

An analytical expression for the classical form factor or impulsive probability $P_{if}(\mathbf{q})$ for $nlm \rightarrow n'l'm$ transitions is derived directly from the ''phase-space distribution'' method [Phys. Rev. A **60**, 1053 (1999)] and is compared with quantal results. Exact universal scaling laws are derived for the classical probability for any $i \rightarrow f$ transition. As n is increased, convergence of the quantal to classical results is obtained and it becomes even more rapid upon averaging in succession over the m and then the l substates. The classical results reveal the basic reason for the underlying structure in the variation of P_{if} with momentum transfer $\mathbf{q}$. Classical form factors can operate as an effective averaged version of the exact quantal counterpart.

DOI: 10.1103/PhysRevA.65.022703 PACS number(s): 32.80.Cy, 34.50.−s, 31.15.Gy

I. INTRODUCTION

State-to-state collisional atomic form factors

$$P_{nlm \rightarrow n'l'm'}(\mathbf{q}) = |\langle \psi_{n'l'm'}(\mathbf{r}) | e^{i\mathbf{q}\cdot\mathbf{r}/\hbar} | \psi_{nlm}(\mathbf{r}) \rangle|^2 \quad (1)$$

are important in theoretical analysis of experiments involving initially oriented or aligned target atoms. Equation (1) is the probability [1,2] for transitions induced by an impulsive perturbation generated, for example, by a short unipolar electromagnetic pulse [3–5] or by sudden collisions with an aligned neutral atom [6–10]. The internal momentum $\mathbf{p}_i$ of the target system with wave function $\psi_i = \psi_{nlm}$ increases impulsively by $\mathbf{q}$ to the momentum $\mathbf{p}_f = \mathbf{p}_i + \mathbf{q}$, of the final state $\psi_f = \psi_{n'l'm'}$. The form factor (1) is also important to the analysis of high angular momentum l states in cold Rydberg gases [11] and in theories [12] of atomic collisions with Rydberg atoms.

There are several ways to create an unbalanced population of magnetic substates in target atoms, e.g., by application of a polarized laser, a weak external static field, or a unidirectional electromagnetic field pulse. The quantum numbers (nlm) appropriate to spherical coordinates can then be used to specify the initial and final states and Eq. (1) is used directly. This is in contrast to experiments [4] with very high n Rydberg atoms in strong external fields when parabolic quantum numbers must be used, since angular momentum is not a conserved quantity.

Highly oscillatory wave functions for the Rydberg electron render unfeasible the direct numerical calculation of the quantal form factor, particularly for $n \geqslant 40$. The classical limit is, however, well defined [1] and provides [13], in the limit of large quantum numbers, good agreement for $nl \rightarrow n'l'$, $nl \rightarrow n'$, and $n \rightarrow n'$ transitions. Classical [14] and quantal [15,16] form factors for transitions between parabolic quantum numbers are available. On writing the $\exp(i\mathbf{q}\mathbf{r}/\hbar)$ operator in terms of the generators for SO(4,2) noncompact symmetry group of the hydrogen atom [16], the quantal form factor has been derived in an elegant fashion for $nlm \rightarrow n'lm$ transitions, with $\Delta l = 0$ and $\Delta m = 0$.

When $\hat{\mathbf{q}}$ is taken as the quantization axis of the system, as in electromagnetic field pulse experiments, Eq. (1) is nonzero only for transitions with $\Delta m \equiv m' - m = 0$. This is also true classically since the projection

$$\mathbf{L}_f \cdot \hat{\mathbf{q}} = \mathbf{r} \cdot (\mathbf{p}_f \times \hat{\mathbf{q}}) = \mathbf{L}_i \cdot \hat{\mathbf{q}}$$

of the final $\mathbf{L}_f = \mathbf{r} \times \mathbf{p}_f$ angular momentum along the momentum-change direction $\hat{\mathbf{q}}$ equals the corresponding projection of the initial $\mathbf{L}_i = \mathbf{r} \times \mathbf{p}_i$ angular momentum.

In this paper, the phase-space distribution (PSD) method previously presented [13] for $nl \rightarrow n'l'$ transitions is extended to provide an analytic expression for the classical form factor for $nlm \rightarrow n'l'm$ transitions in a Rydberg atom for a general electron-core interaction $V(r)$. The derived expression agrees with that deduced by Bersons *et al.* [17] from a different approach based on the kinematics of an electron moving in an elliptical orbit under Coulomb attraction. An advantage of the present PSD method is that general classical scaling laws can immediately be derived in transparent form. These are then used to explore the convergence of the quantal form factors onto the classical background as the principal quantum number n is increased. This convergence is important for cases when n is very large ($n \simeq 400$ in half-cycle experiments of Bromage and Stroud [4]) where accurate quantal calculations are unfeasible, if not impossible. Reliance on the use of classical form factors must, therefore, be established and justified for state-to-state transitions, as here.

II. PHASE-SPACE DISTRIBUTION METHOD

The quantal probability (1) for transitions in which momentum $\mathbf{q}$ is impulsively transferred to the target particle can be rewritten [1] as

$$P_{if}(\mathbf{q}) = (2\pi\hbar)^3 \frac{\int \rho_i(\mathbf{r},\mathbf{p}) \rho_f(\mathbf{r},\mathbf{p}+\mathbf{q}) d\mathbf{r} d\mathbf{p}}{\int \rho_i(\mathbf{r},\mathbf{p}) d\mathbf{r} d\mathbf{p}}, \quad (2)$$

where quantal densities

$$\rho_j^q(\mathbf{r},\mathbf{p}) = (2\pi\hbar)^{-3/2} \phi_j^*(\mathbf{p}) \exp(-i\mathbf{p}\cdot\mathbf{r}/\hbar) \psi_j(\mathbf{r}) \quad (3)$$

are expressed in terms of the spatial and momentum wave functions $\psi_j(\mathbf{r})$ and $\phi_j(\mathbf{p})$, respectively for the initial i and final f states. This function (3), which is the standard ordered version of the Wigner PSD, is normalized to unity and may be interpreted as the quantal PSD. The probability

$$\mathcal{P}_{if}(\mathbf{q}) = (2\pi\hbar)^3 \int \rho_i(\mathbf{r},\mathbf{p})\rho_f(\mathbf{r},\mathbf{p}+\mathbf{q})d\mathbf{r}d\mathbf{p} \tag{4}$$

from all degenerate states i with statistical weights

$$g_i = \int \rho_i(\mathbf{r},\mathbf{p})d\mathbf{r}d\mathbf{p}$$

satisfies detailed balance $\mathcal{P}_{if}(\mathbf{q}) = \mathcal{P}_{fi}(-\mathbf{q})$ and is symmetric in i and f.

A. Classical distributions

The volume of phase space occupied by particles moving under Hamiltonian $H = p^2/2m + V(r)$ in a symmetrical potential $V(r)$ with specified energy E, angular momentum $\mathbf{L} = \mathbf{r}\times\mathbf{p}$ and L_z, its component along a fixed direction $\hat{\mathbf{z}}$ of atomic quantization, in the range $dEdLdL_z$ centered about (E,L,L_z) is

$$\begin{aligned}\mathcal{V}_{ELL_z} = dEdLdL_z \int \delta(H(r,p)-E)\delta(|\mathbf{r}\times\mathbf{p}|-L) \\ \times \delta((\mathbf{r}\times\mathbf{p})\cdot\hat{\mathbf{z}}-L_z)d\mathbf{r}d\mathbf{p} \\ = \mathcal{V}_{nlm}dndldm.\end{aligned} \tag{5}$$

The number of bound nlm states within volume $\mathcal{V}_{nlm}$ is

$$g_{nlm} \equiv \frac{\mathcal{V}_{nlm}}{(2\pi\hbar)^3} = \int \rho^c_{nlm}(\mathbf{r},\mathbf{p})d\mathbf{r}d\mathbf{p}. \tag{6}$$

The classical PSD of nlm states is therefore

$$\begin{aligned}\rho^c_{nlm}(\mathbf{r},\mathbf{p}) = \frac{1}{(2\pi\hbar)^3}\left(\frac{dE}{dn}\right)\left(\frac{dL}{dl}\right)\left(\frac{dL_z}{dm}\right)\delta(H(r,p)-E) \\ \times \delta(|\mathbf{r}\times\mathbf{p}|-L)\,\delta((\mathbf{r}\times\mathbf{p})\cdot\hat{\mathbf{z}}-L_z),\end{aligned} \tag{7}$$

which, upon integration, yields

$$g_{nlm} = \frac{1}{(2\pi\hbar)^3}\left(\frac{dE}{dn}\right)\left(\frac{dL}{dl}\right)\left(\frac{dL_z}{dm}\right)\left(\frac{8\pi^3}{\omega_{nl}}\right)$$

for the number (6) of bound nlm states. The angular frequency for bounded radial motion is given, in terms of the radial action, by $\omega_{nl} \equiv 2\pi\partial H/\partial J$. Under the substitutions, $dE/dn = \hbar\omega_{nl}$, $dL/dl = \hbar$ and $dL_z/dm = \hbar$, for the spacings between neighboring states, the phase volume is $\mathcal{V}_{nlm} = (2\pi\hbar)^3$ and the number of states $g_{nlm} = 1$. The corresponding nlm one-particle PSD is then

$$\begin{aligned}\rho^c_{nlm}(\mathbf{r},\mathbf{p}) = \frac{\hbar\omega_{nl}}{(2\pi\hbar)^3}\delta(H(r,p)-E)\,\hbar\,\delta(|\mathbf{r}\times\mathbf{p}|-L) \\ \times \hbar\,\delta((\mathbf{r}\times\mathbf{p})\cdot\hat{\mathbf{z}}-L_z),\end{aligned} \tag{8}$$

which is normalized to one particle. The volume of phase space occupied by particles in state nl is

$$\mathcal{V}_{nl} = \left(\frac{dE}{dn}\right)\left(\frac{dL}{dl}\right)\int \delta(H(r,p)-E)\delta(|\mathbf{r}\times\mathbf{p}|-L)d\mathbf{r}d\mathbf{p}. \tag{9}$$

The degeneracy g_{nl} is $(2\pi\hbar)^{-3}\mathcal{V}_{nl} = 2l$. The classical PSD appropriate to these $2l$ bound nl states is then

$$\rho^c_{nl}(\mathbf{r},\mathbf{p}) = \frac{\hbar\omega_{nl}}{(2\pi\hbar)^3}\delta(H(r,p)-E)\hbar\,\delta(|\mathbf{r}\times\mathbf{p}|-L). \tag{10}$$

The classical PSD appropriate to the degenerate $g_n = n^2$ bound hydrogenic states within level n is similarly

$$\rho^c_n(\mathbf{r},\mathbf{p}) = \frac{\hbar\omega_n}{(2\pi\hbar)^3}\delta(H(r,p)-E). \tag{11}$$

The classical correspondence with Eq. (2) may now be established.

B. Classical-quantal probability correspondence

The phase-space volume occupied by those final $(n'l')$ states that can be accessed only from the initial distribution of (nl) states via an impulsive transfer of momentum $\mathbf{q}$ at electronic separation $\mathbf{r}$ is

$$\begin{aligned}\mathcal{V}_{nl,n'l'}(\mathbf{q}) = \left(\frac{dE_i}{dn}\frac{dL_i}{dl}\frac{dE_f}{dn'}\frac{dL_f}{dl'}\right)\int d\mathbf{r}d\mathbf{p}\{\delta(H(r,p) \\ -E)\delta(|\mathbf{r}\times\mathbf{p}|-L)\}\{\delta(\mathbf{r}'-\mathbf{r})\,\delta(\mathbf{p}'-(\mathbf{p}+\mathbf{q}))\} \\ \times\{\delta(H(r',p')-E') \\ \times \delta(|\mathbf{r}'\times\mathbf{p}'|-L')\}d\mathbf{r}'d\mathbf{p}'.\end{aligned} \tag{12}$$

The number $g_{nl,n'l'}$ of final $(n'l')$ states originating from the (nl) states is $\mathcal{V}_{nl,n'l'}/(2\pi\hbar)^3$. The classical probability for transitions from one initial state to the band of final states is then the ratio

$$P_{nl,n'l'} = g_{nl,n'l'}/g_{nl} = \mathcal{V}_{nl,n'l'}/\mathcal{V}_{nl} \tag{13}$$

of final to initial populations or, alternatively, the ratio of the overlap phase volume (12) to the initial volume (9). The classical probability for $nl \to n'l'$ transitions can therefore be expressed in terms of the classical PSD (10) for bound states by

$$P^c_{nl,n'l'}(\mathbf{q}) = (2\pi\hbar)^3 \int \rho^c_{nl}(\mathbf{r},\mathbf{p})\rho^c_{n'l'}(\mathbf{r},\mathbf{p}+\mathbf{q})d\mathbf{r}d\mathbf{p} \Big/ \int \rho^c_{nl}(\mathbf{r},\mathbf{p})d\mathbf{r}d\mathbf{p}. \tag{14}$$

Comparison between Eqs. (14) and (2), therefore, establishes directly the classical-quantal correspondence between the impulsive probabilities given as the normalized overlap of the corresponding initial and final PSD's. The probability for transitions from the degenerate $g_{nl}=2l$ initial states i to the $2l'$ final states f is the overlap

$$\mathcal{P}^c_{nl,n'l'}(\mathbf{q}) \equiv g_{nl}P^c_{nl,n'l'}(\mathbf{q}) = (2\pi\hbar)^3 \int \rho^c_{nl}(\mathbf{r},\mathbf{p})\rho^c_{n'l'}(\mathbf{r},\mathbf{p}+\mathbf{q})d\mathbf{r}d\mathbf{p},$$

which also satisfies the relation $\mathcal{P}^c_{nl,n'l'}(+\mathbf{q}) = \mathcal{P}^c_{n'l',nl}(-\mathbf{q})$ for a detailed balance. The classical probability for transitions from the degenerate n^2 initial states in level n of hydrogenic atoms to the n'^2 final states in level n' is

$$\mathcal{P}^c_n(\mathbf{q}) = (2\pi\hbar)^3 \int \rho^c_n(\mathbf{r},\mathbf{p})\rho^c_{n'}(\mathbf{r},\mathbf{p}+\mathbf{q})d\mathbf{r}\,d\mathbf{p}.$$

C. State-to-state transition probabilities

The classical probability (form factor) for $i \equiv nlm \to f \equiv n'l'm'$ transitions is

$$P_{nlm,n'l'm'}(\mathbf{q}) = \frac{1}{(2\pi\hbar)^3}\left(\frac{dE_i}{dn}\frac{dL_i}{dl}\frac{dL_{iz}}{dm}\frac{dE_f}{dn'}\frac{dL_f}{dl'}\frac{dL_{fz}}{dm'}\right)V_{nlm,n'l'm'}(\mathbf{q}) \tag{15}$$

in terms of the overlapped volume density (of initial and final states),

$$V_{if}(\mathbf{q}) = \int \delta(H(r,p)-E_i)\delta(|\mathbf{r}\times\mathbf{p}|-L_i) \times \delta(H(r,|\mathbf{p}+\mathbf{q}|)-E_f)\delta(|\mathbf{r}\times(\mathbf{p}+\mathbf{q})|-L_f) \times \delta((\mathbf{r}\times\mathbf{p})\cdot\hat{\mathbf{z}}-L_{iz})\delta([\mathbf{r}\times(\mathbf{p}+\mathbf{q})]\cdot\hat{\mathbf{z}}-L_{fz})d\mathbf{r}d\mathbf{p}, \tag{16}$$

which is simply the phase-space overlap integral of δ functions involving states $i=(E_i,L_i,L_{iz})$ and $f=(E_f,L_f,L_{fz})$. This overlap is illustrated in Fig. 1. Evolution to the final-state manifold is achieved via the allowed phase-space trajectories indicated.

For hydrogenic states, $E=\epsilon_0/2n^2, L=l\hbar, L_z=m\hbar$ where ϵ_0 is the atomic unit of energy, and the transition probability is obtained upon setting $dE/dn=\hbar\omega_n=\epsilon_0/n^3$, $dL/dl=\hbar$, and $dL_z/dm=\hbar$ to give

$$P_{nlm,n'l'm'}(\mathbf{q}) = \frac{\epsilon_0^2\hbar}{8\pi^3 n^3 n'^3}V_{nlm,n'l'm'}(\mathbf{q}) \tag{17}$$

in terms of the volume density (16). The probabilities for $nl\to nl'$ and in $n\to n'$ transitions from all degenerate initial levels are

$$\mathcal{P}_{nl,n'l'}(\mathbf{q}) = \frac{(\epsilon_0^2/\hbar)}{8\pi^3 n^3 n'^3}V_{nl,n'l'}(\mathbf{q}) \tag{18}$$

and

$$\mathcal{P}_{n,n'}(\mathbf{q}) = \frac{(\epsilon_0^2/\hbar^3)}{8\pi^3 n^3 n'^3}V_{n,n'}(\mathbf{q}), \tag{19}$$

respectively, in terms of the corresponding volume densities

$$V_{nl,n'l'}(\mathbf{q}) = \int \delta(H(r,p)-E_i)\delta(|\mathbf{r}\times\mathbf{p}|-L_i) \times \delta(H(r,|\mathbf{p}+\mathbf{q}|)-E_f)\delta(|\mathbf{r}\times(\mathbf{p}+\mathbf{q})|-L_f)d\mathbf{r}d\mathbf{p} \tag{20}$$

and

$$V_{n,n'}(\mathbf{q}) = \int \delta(H(r,p)-E_i)\delta(H(r,|\mathbf{p}+\mathbf{q}|)-E_f)d\mathbf{r}d\mathbf{p}, \tag{21}$$

respectively.

D. Classical scaling rules

An advantage of the classical formulation above is that very useful universal scaling laws for the probabilities can be derived. On introducing a scaling factor α, such that $p'=\alpha p$ and $r'=r/\alpha^2$ for hydrogenic systems, then $H' \equiv H(p',r')=\alpha^2 H(p,r)$, $E'=\alpha^2 E$ and $\mathbf{L}'=\mathbf{r}'\times\mathbf{p}'=\mathbf{L}/\alpha$. It follows that the continuum PSD

$$\rho^c_{ELL_z}(\mathbf{r},\mathbf{p}) = (2\pi\hbar)^{-3}dE\,dL\,dL_Z\delta(H-E)\,\delta(|\mathbf{r}\times\mathbf{p}|-L) \times \delta(\mathbf{L}\cdot\hat{\mathbf{z}}-L_z) \tag{22}$$

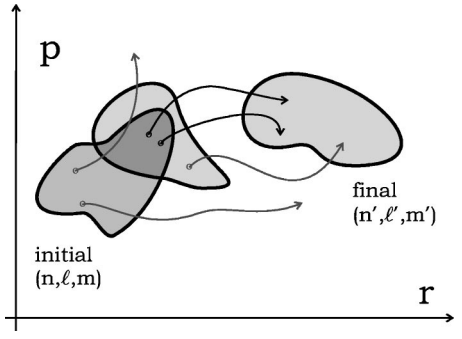

FIG. 1. Classical form factor is a ratio of two phase-space volumes: the volume of the region within that part of the initial-state manifold containing coordinates that can evolve into the final-state manifold, and the total volume of the initial-state manifold.

and the associated L_z and (L_z,L) integrated PSD's, ρ^c_{EL} and ρ^c_E, therefore scale as

$$\rho^c_\Gamma(\mathbf{r},\mathbf{p}) = \rho^c_{\Gamma'}(\mathbf{r}',\mathbf{p}'),$$

an invariant for all sets $\Gamma \equiv (ELL_z),(EL),E$. For continuum-continuum transitions, the symmetric probabilities

$$\mathcal{P}_{\Gamma_i,\Gamma_f}(\mathbf{q}) = (2\pi\hbar)^3 \int \rho^c_{\Gamma_i}(\mathbf{r},\mathbf{p})\rho^c_{\Gamma_f}(\mathbf{r},\mathbf{p}+\mathbf{q})d\mathbf{r}\,d\mathbf{p}$$

therefore scale, independently of Γ, as

$$\mathcal{P}_{\Gamma_i,\Gamma_f}(\mathbf{q}) = \alpha^3 \mathcal{P}_{\Gamma_i,\Gamma_f}(\mathbf{q}'),$$

where $\mathbf{q}' = \alpha\mathbf{q}$. Since $n = \alpha n'$, $l = \alpha l'$ and $m = \alpha m'$, the bound state PSD's (8), (10) and (11) however scale according to

$$\rho^c_{nlm}(\mathbf{r},\mathbf{p}) = \alpha^{-3}\rho^c_{n'l'm'}(\mathbf{r}',\mathbf{p}'), \tag{23}$$

$$\rho^c_{nl}(\mathbf{r},\mathbf{p}) = \alpha^{-2}\rho^c_{n'l'}(\mathbf{r}',\mathbf{p}'), \tag{24}$$

$$\rho^c_{n}(\mathbf{r},\mathbf{p}) = \alpha^{-1}\rho^c_{n'}(\mathbf{r}',\mathbf{p}'). \tag{25}$$

The probabilities

$$\mathcal{P}_{\Gamma_i,nlm}(\mathbf{q}) = (2\pi\hbar)^3 \int \rho^c_{\Gamma_i}(\mathbf{r},\mathbf{p})\rho^c_{nlm}(\mathbf{r},\mathbf{p}+\mathbf{q})d\mathbf{r}\,d\mathbf{p}$$

for continuum-bound (recombination) transitions therefore scale as

$$\mathcal{P}_{ELL_z,nlm}(\mathbf{q}) = \mathcal{P}_{E'L'L'_z,n'l'm'}(\mathbf{q}'), \tag{26}$$

$$\mathcal{P}_{EL,nl}(\mathbf{q}) = \alpha\mathcal{P}_{E'L',n'l'}(\mathbf{q}'), \tag{27}$$

$$\mathcal{P}_{E,n}(\mathbf{q}) = \alpha^2\mathcal{P}_{E',n'}(\mathbf{q}'). \tag{28}$$

The probabilities for bound-bound transitions

$$\mathcal{P}_{if}(\mathbf{q}) = g_i P_{if} = (2\pi\hbar)^3 \int \rho_i(\mathbf{r},\mathbf{p})\rho_f(\mathbf{r},\mathbf{p}+\mathbf{q})d\mathbf{r}d\mathbf{p} \tag{29}$$

from the g_i initial states scale as

$$P_{n_il_im_i,n_fl_fm_f}(\mathbf{q}) = \alpha^{-3}P_{n'_il'_im'_i,n'_fl'_fm'_f}(\mathbf{q}'), \tag{30}$$

$$P_{n_il_im_i,n_fl_f}(\mathbf{q}) = \alpha^{-2}P_{n'_il'_im'_i,n'_fl'_f}(\mathbf{q}'), \tag{31}$$

$$\mathcal{P}_{n_il_i,n_fl_f}(\mathbf{q}) = \alpha^{-1}\mathcal{P}_{n'_il'_i,n'_fl'_f}(\mathbf{q}'), \tag{32}$$

$$\mathcal{P}_{n_il_i,n_f}(\mathbf{q}) = \alpha^{0}\mathcal{P}_{n'_il'_i,n'_f}(\mathbf{q}'), \tag{33}$$

$$\mathcal{P}_{n_i,n_f}(\mathbf{q}) = \alpha\mathcal{P}_{n'_i,n'_f}(\mathbf{q}'). \tag{34}$$

Summation over the initial/final substates is implied when the corresponding quantum numbers do not appear as subscripts.

Applications

(A) By choosing $\alpha = n_i$, for example, it can then be shown that the $i \to f$ symmetric probabilities (30)–(34) written as $\mathcal{P}(i;f;\mathbf{q})$ satisfy the rules

$$n_i^3 P(n_il_im_i;n_fl_fm_f;\mathbf{q}/n_i) = P(1,\epsilon_i,\mu_i;\eta_f,\epsilon_f,\mu_f;\mathbf{q}), \tag{35}$$

$$n_i^2 P(n_il_im_i;n_fl_f;\mathbf{q}/n_i) = P(1,\epsilon_i,\mu_i;\eta_f,\epsilon_f,\mu_i;\mathbf{q}), \tag{36}$$

$$n_i \mathcal{P}(n_il_i;n_fl_f;\mathbf{q}/n_i) = \mathcal{P}(1,\epsilon_i;\eta_f,\epsilon_f;\mathbf{q}), \tag{37}$$

$$n_i^{-1}\mathcal{P}(n_i;n_f;\mathbf{q}/n_i) = \mathcal{P}(1;\eta_f;\mathbf{q}), \tag{38}$$

where the parameters are $\epsilon_j = l_j/n_i$, $\mu_j = m_j/n_i$ and $\eta_f = n_f/n_i$. The transition arrays for *all* n_i can, therefore, be deduced from the array from a single value of n_i, e.g., $n_i = 1$. The dimensionality of the transition arrays is then reduced by one.

(B) The quasielastic transition arrays $(n_il_im_i \to n_il_fm_f)$ and $(n_il_i \to n_il_f)$ can be scaled similarly by choosing $\alpha = l_i$ to provide the rules

$$l_i^3 P(n_il_im_i;n_il_fm_f;\mathbf{q}/l_i) = P(\beta_i,1,\delta_i;\beta_i\gamma_f\delta_f;\mathbf{q}), \tag{39}$$

$$l_i \mathcal{P}(n_il_i;n_il_f;\mathbf{q}/l) = \mathcal{P}(\beta_i,1;\beta_i\gamma_f\delta_f;\mathbf{q}), \tag{40}$$

where $\beta_i = n_i/l_i$, $\gamma_f = l_f/l_i$, and $\delta_j = m_j/l_i$.

III. ANALYTICAL EXPRESSION FOR THE PROBABILITY

The volume density phase-space integration (16) for state-to-state transitions is accomplished by noting that the δ functions of the initial and final Hamiltonians, $H_i = p^2/2\mu + V(r)$ and $H_f = |\mathbf{p}+\mathbf{q}|^2/2\mu + V(r)$, are

$$\delta(H_i - E_i) = (\mu/p)\,\delta(p - [2\mu(E_i - V(r))]^{1/2}), \tag{41}$$

$$\delta(H_f - E_f) = (\mu/pq)\,\delta\left[\cos\chi - \frac{E_f - H_i - q^2/2\mu}{pq/\mu}\right], \tag{42}$$

where χ is the angle between $\mathbf{p}$ and $\mathbf{q}$ such that

$$H_f(\mathbf{p},\mathbf{r}) = \frac{p^2 + 2\mathbf{p}\cdot\mathbf{q} + q^2}{2\mu} + V(r) = H_i + \frac{q^2}{2\mu} + \frac{pq}{\mu}\cos\chi.$$

It now proves extremely advantageous to adopt the spherical bifocal coordinates u_i and u_f introduced previously in Ref. [18] and represented in Fig. 2. The δ functions of the angular momentum are

$$\delta(|\mathbf{r}\times\mathbf{p}| - L_i) = \frac{\delta(u_i - U_i) + \delta(u_i - (\pi - U_i))}{rp|\cos U_i|}, \tag{43}$$

$$\delta(|\mathbf{r}\times(\mathbf{p}+\mathbf{q})| - L_f) = \frac{\delta(u_f - U_f) + \delta(u_f - (\pi - U_f))}{r|\mathbf{p}+\mathbf{q}||\cos U_f|}, \tag{44}$$

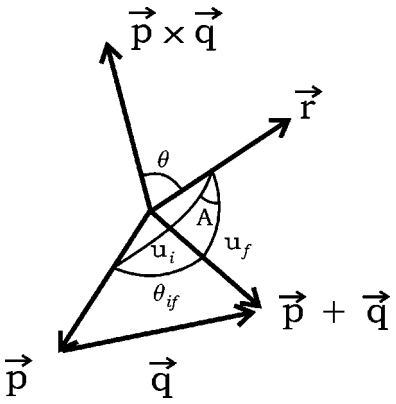

FIG. 2. Basic geometry involved in the calculation of the classical state-to-state form factor.

where the angles u_j are determined by $\cos u_i = \hat{\mathbf{r}}\cdot\hat{\mathbf{p}}$ and $\cos u_f = \hat{\mathbf{r}}\cdot\widehat{(\mathbf{p}+\mathbf{q})}$. Also

$$\sin U_i = \frac{L_i}{rp}; \quad \sin U_f = \frac{L_f}{r|\mathbf{p}+\mathbf{q}|}.$$

The phase-space volume element can then be expressed [18] in terms of the u_i and u_f in Fig. 2 as

$$d\mathbf{p}\,d\mathbf{r} = [p^2 dp d(\cos\theta_p) d\phi_p]\left\{\frac{2du_i du_f}{\sin A}\right\} r^2 dr,$$

where (θ_p, ϕ_p) are the polar and azimuthal angles of $\mathbf{p}$ relative to a fixed set of axis and where A is determined from

$$\cos A = \frac{p^2 + |\mathbf{p}+\mathbf{q}|^2 - q^2 - 2p|\mathbf{p}+\mathbf{q}|\cos u_i \cos u_f}{2p|\mathbf{p}+\mathbf{q}|\sin u_i \sin u_f}.$$

Subsequent calculation of Eq. (16) or Eq. (20) depends on whether or not there is a fixed direction of space as specified by an electric or magnetic field.

(a) When no fixed axis is specified, then θ_p can be identified with the angle χ between $\mathbf{p}$ and $\mathbf{q}$. Under the constraints (41)–(45), $p|\mathbf{p}+\mathbf{q}||\cos u_i||\cos u_f| = \mu^2 R_i R_f$, where the radial speeds $R_{i,f}(r) = \dot{r}_{i,f}$ are determined from energy conservation

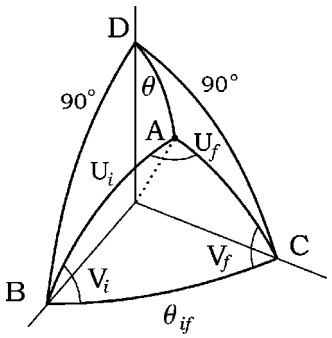

FIG. 3. In spherical bifocal coordinates, point A is identified by angles U_i and U_f of arcs BA and CA on the unit sphere. The area element is $dS = dU_i dU_f / \sin A$, where A is the angle between arcs BA and CA.

$$E_{i,f} = \frac{1}{2}\mu \dot{r}_{i,f}^2 + V(r) + \frac{L_{i,f}^2}{2\mu r^2} \tag{45}$$

as functions only of r for specified energy and angular momentum. The phase-space integrations in the volume density (20) for $nl \to n'l'$ transitions can then be performed directly to yield

$$\begin{aligned} V_{nl,n'l'}(\mathbf{q}) &= \frac{8\pi}{q}\int_{\mathcal{R}} \frac{dr}{R_i(r)R_f(r)}\left[\frac{1}{\sin A_+} + \frac{1}{\sin A_-}\right]\Theta(r,q) \\ &= \frac{16\pi L_i L_f}{q}\int_{\mathcal{R}} \frac{dr/r^2}{R_i(r)R_f(r)} \\ &\quad \times\left\{\left[\frac{4L_i^2 L_f^2}{r^4} - C_+^2(r)\right]^{-1/2} \right. \\ &\quad \left. + \left[\frac{4L_i^2 L_f^2}{r^4} - C_-^2(r)\right]^{-1/2}\right\}\Theta(r,q), \end{aligned} \tag{46}$$

where quantities $C_\pm$ are defined as

$$\begin{aligned} C_\pm(r) &= 2\mu[E_i + E_f - 2V(r)] \pm 4\mu\left[E_i - V(r) - \frac{L_i^2}{r^2}\right]^{1/2} \\ &\quad \times\left[E_f - V(r) - \frac{L_f^2}{r^2}\right]^{1/2} - q^2 \\ &= \mu^2[R_i(r) \pm R_f(r)]^2 + \frac{(L_i^2 + L_f^2)}{r^2} - q^2. \end{aligned}$$

The step function Θ is unity provided $V(r) \leqslant E_i - \mu(E_f - E_i - q^2/2\mu)^2/2q^2$ and zero otherwise. The region $\mathcal{R}$ of radial integration, within which $A_\pm$ are real, is determined by the condition $C_\pm^2(r) \leqslant 4L_i^2 L_f^2/r^4$. The above result (46) is identical with that calculated previously [13] via a different integration method. The integrand of Eq. (46) is an ingredient [12] in classical impulsive theories of $A-B(nl)$ collisions when the cross section $\sigma(g,q)$ for scattering of the Rydberg electron by A at relative speed g is a function of both g and the momentum q transferred. When σ is a function only of q, the full integral (46) is then applicable [12].

(b) For transitions between m sublevels, there is a fixed direction of atomic quantization and the calculation is more difficult. The δ function involving L_{fz} is

$$\delta([\mathbf{r}\times(\mathbf{p}+\mathbf{q})]\cdot\hat{\mathbf{z}} - L_{fz}) = \delta(\mathbf{r}\cdot(\mathbf{q}\times\hat{\mathbf{z}}) - (L_{fz} - L_{iz})), \tag{47}$$

where $\mathbf{q}\times\hat{\mathbf{z}}$ is a fixed direction in space. For the impulse $\mathbf{q}$ directed along the quantization axis $\hat{\mathbf{z}}$, then (47) reduces to $\delta(L_{fz} - L_{iz})$ and only transitions with $L_{iz} = L_{fz} \equiv L_z$ occur. Moreover, the azimuthal angle ϕ_p of $\mathbf{p}$ may now rotate freely in the range $[0 - \pi]$ and $\mathbf{r}$, for fixed U_i and U_f, is attached to the rotated $\mathbf{p}$. With the aid of the spherical bifocal coordinates [18], it can be shown (see Fig. 3 as well as the Appendix) that the δ function of L_{iz} in Eq. (16) reduces to

$$\delta((\mathbf{r}\times\mathbf{p})\cdot\hat{\mathbf{z}}-L_{iz})=\delta\left(\frac{L_iL_f}{qr}\sin A-L_{iz}\right). \tag{48}$$

Under the conditions (41)–(43), it can be expressed as

$$\begin{aligned}&\delta((\mathbf{r}\times\mathbf{p})\cdot\hat{\mathbf{z}}-L_{iz})\\&=\frac{8q^2L_z}{r^2}\delta\left(C_{\pm}^2(r)+\left(\frac{2qL_z}{r}\right)^2-\left(\frac{2L_iL_f}{r^2}\right)^2\right)\\&=\frac{8q^2L_z}{r^2}\left\{\sum_k\frac{\delta(r-r_k)}{|\partial F_{\pm}(r_k)/\partial r|}\right\},\end{aligned} \tag{49}$$

where the summation includes all roots r_k of

$$F_{\pm}(r;q)=C_{\pm}^2(r)+\left(\frac{2qL_z}{r}\right)^2-\left(\frac{2L_iL_f}{r^2}\right)^2=0,$$

where the $nlm\rightarrow n'l'm$ transitions occur classically. The sixfold integration in the probability (17) for $nlm\rightarrow n'l'm$ transitions resulting from the impulse $\hbar\mathbf{q}$ directed along the z axis of atomic quantization then reduces to the following exact result:

$$\begin{aligned}&P_{nlm\rightarrow n'l'm}(\mathbf{q})\\&=\frac{(2l)(2l')}{\pi^2n^3n'^3}(\hbar\epsilon_0^2)\sum_k\frac{1}{|r_k^3R_i(r_k)R_f(r_k)\partial F_{\pm}(r_k)/\partial r|},\end{aligned} \tag{50}$$

where ϵ_0 is the atomic unit of energy. This result reduces to that in Ref. [17] for Coulomb attraction and, when summed over m to the earlier result [13] for $nl\rightarrow n'l'$ transitions. There are always two or four roots r_k. When two roots accidentally coalesce, where $\partial F_{\pm}(r)/\partial r$ vanishes, the classical transition probability has a singularity. The basic variation of the classical form factor (50) with q for the $n=5,l=4,m=1\rightarrow 8,2,1$ transition in atomic hydrogen is displayed in Fig. 4, together with the q-variation of corresponding roots $r_k(q)$, given by the intersection of the surfaces $z=F_{\pm}(r;q)$ with the $z=0$ plane. It is seen that cusp singularities are exhibited in $P_{nlm\rightarrow n'l'm}(q)$ when the line $q=$const is tangential to the $r_k(q)$ curves . This occurs at four places in Fig. 4. The magnitude of the probability between the singularities is proportional to the number k of contributing radial roots where the m transitions occur. The probabilities $P_{nlm\rightarrow n'l'm}(q)$ are, of course, zero in the classical inaccessible region shown.

The probability (50) obeys the following scaling law:

$$n^2P_{nlm\rightarrow n'l'm}(\mathbf{q}/n)=P_{1,l/n,m/n\rightarrow n'/n,l'/n,m/n}(q),$$

cf. Eq. (36), which will be used to explore the quantal-classical convergence as n is increased.

IV. QUANTAL FORM FACTOR

Here, a numerical technique is devised for accurate calculation of the quantal form factor, even for high $n\sim 100$. An analytic expression for the quantal form factor (1) can be

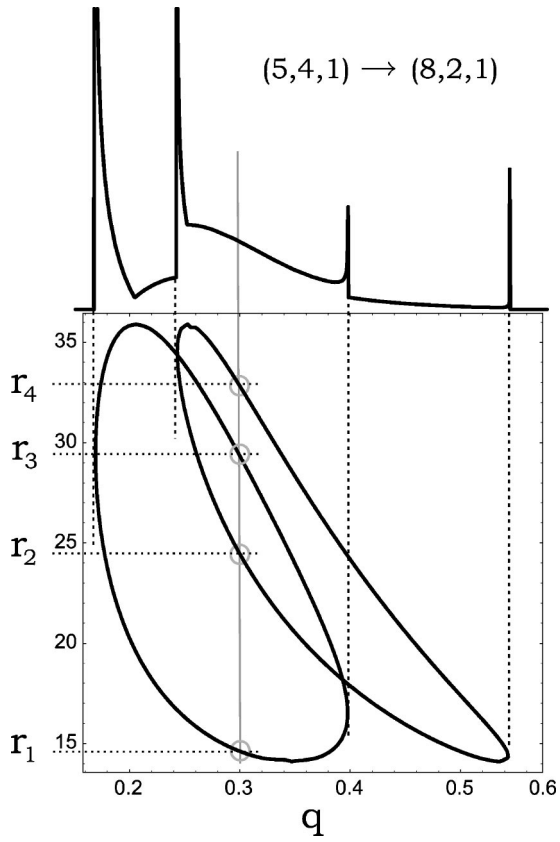

FIG. 4. Contour lines for equation $F_{\pm}(r;q)=0$ in the $q-r$ plane. In the upper part of the diagram, classical probability for transition $(n=5,l=4,m=1)\rightarrow(n'=8,l'=2,m'=1)$. Singularities arise when two roots r_k are equal.

obtained by using the expansion of the exponential function in terms of spherical Bessel functions and spherical harmonics. Upon integration,

$$P^Q_{nlm\rightarrow n'l'm}(q)=\left|\not{\sum}_{k=l+l'+2}^{n+n'}w_kd_k(-q^2/\alpha^2)\right|^2, \tag{51}$$

where the prefactor is

$$\begin{aligned}\not{\ }&=\frac{1}{4\alpha}\sqrt{\frac{2l'+1}{2l+1}}\sqrt{\frac{(n-l-1)!}{(n+l)!}}\\&\times\sqrt{\frac{(n'-l'-1)!}{(n'+l')!}}\left(\frac{2}{n}\right)^{l+2}\left(\frac{2}{n'}\right)^{l'+2}\left(\frac{q}{\alpha}\right)^{|l-l'|},\end{aligned}$$

in terms of $\alpha=1/n+1/n'$. The w_k term is the coefficient of the power r^k in the expansion of the product of radial polynomials

$$(r/\alpha)^2R_{nl}R_{n'l'}=\sum_{k=l+l'+2}^{n+n'}w_kr^k,$$

where

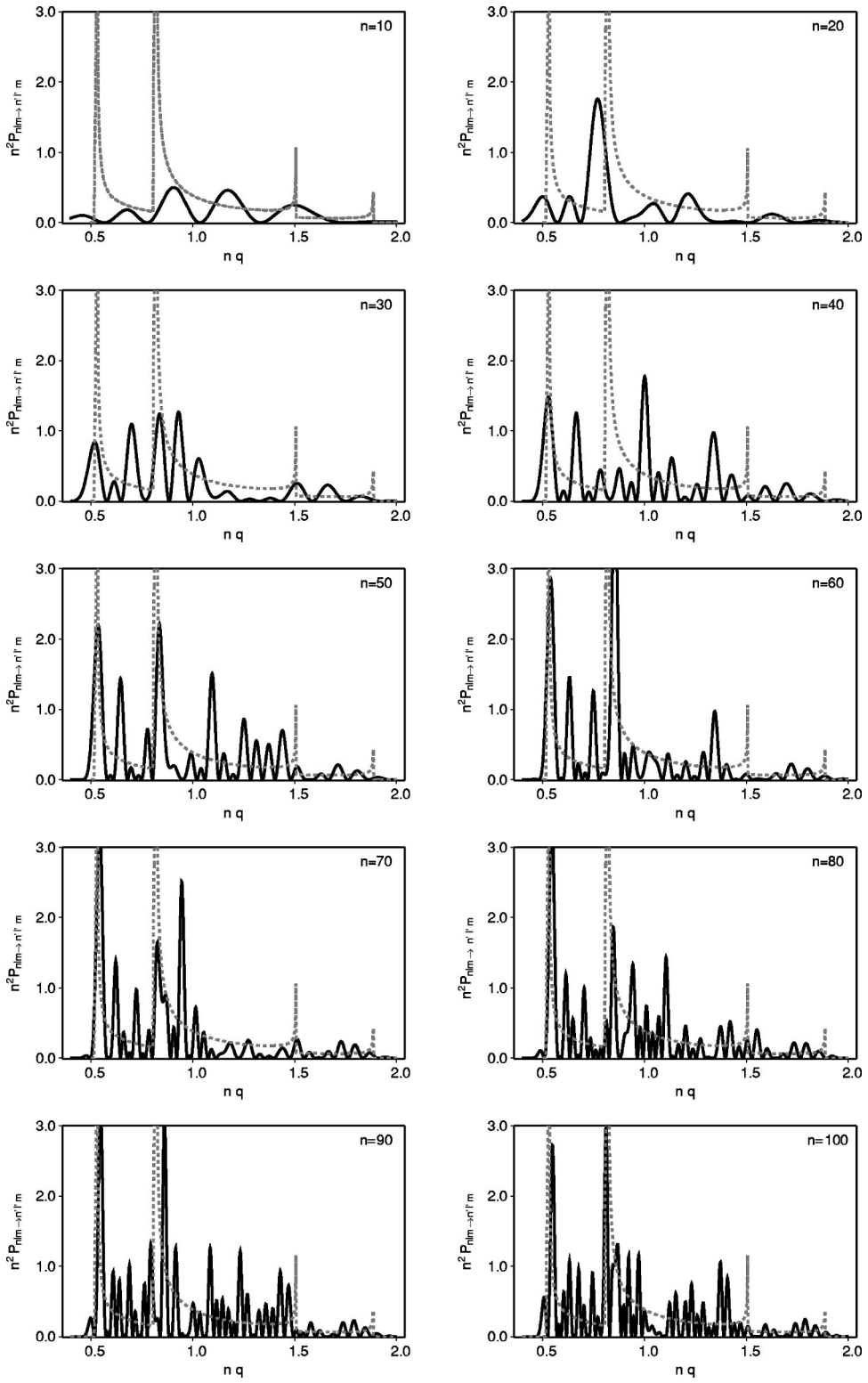

FIG. 5. Classical (dotted line) and quantal (solid line) scaled form factors as a function of scaled momentum transfer $\bar{q}=nq$ for $nlm\to n'l'm$ transitions. For transitions with fixed parameters $l/n=3/10$, $n'/n=14/10$, $l'/n=12/10$, and $m/n=1/10$ convergence is obtained as n is increased from $n=10$ to $n=100$.

$$R_{nl}=(r/\alpha)^l L_{n-l-1}^{(2l+1)}\left(\frac{2r}{n\alpha}\right)$$

is the polynomial part of the radial hydrogenic wave function defined in terms of Laguerre polynomials $L_n^{(a)}(x)$. Finally, the q dependence of the quantal form factor (51) is contained within the functions d_k defined by

$$d_k(x)=\frac{1}{(1-x)^k}\sum_{s=0}^{\min(l,l')} C^{l0}_{l'0L0}C^{lm}_{l'mL0}\frac{(k+L)!}{(2L-1)!!}\times x^s\,{}_2F_1\left[\frac{L-k+1}{2},\frac{L-k}{2}+1,L+3/2;x\right],$$

where C are Clebsch-Gordan coefficients for the addition of

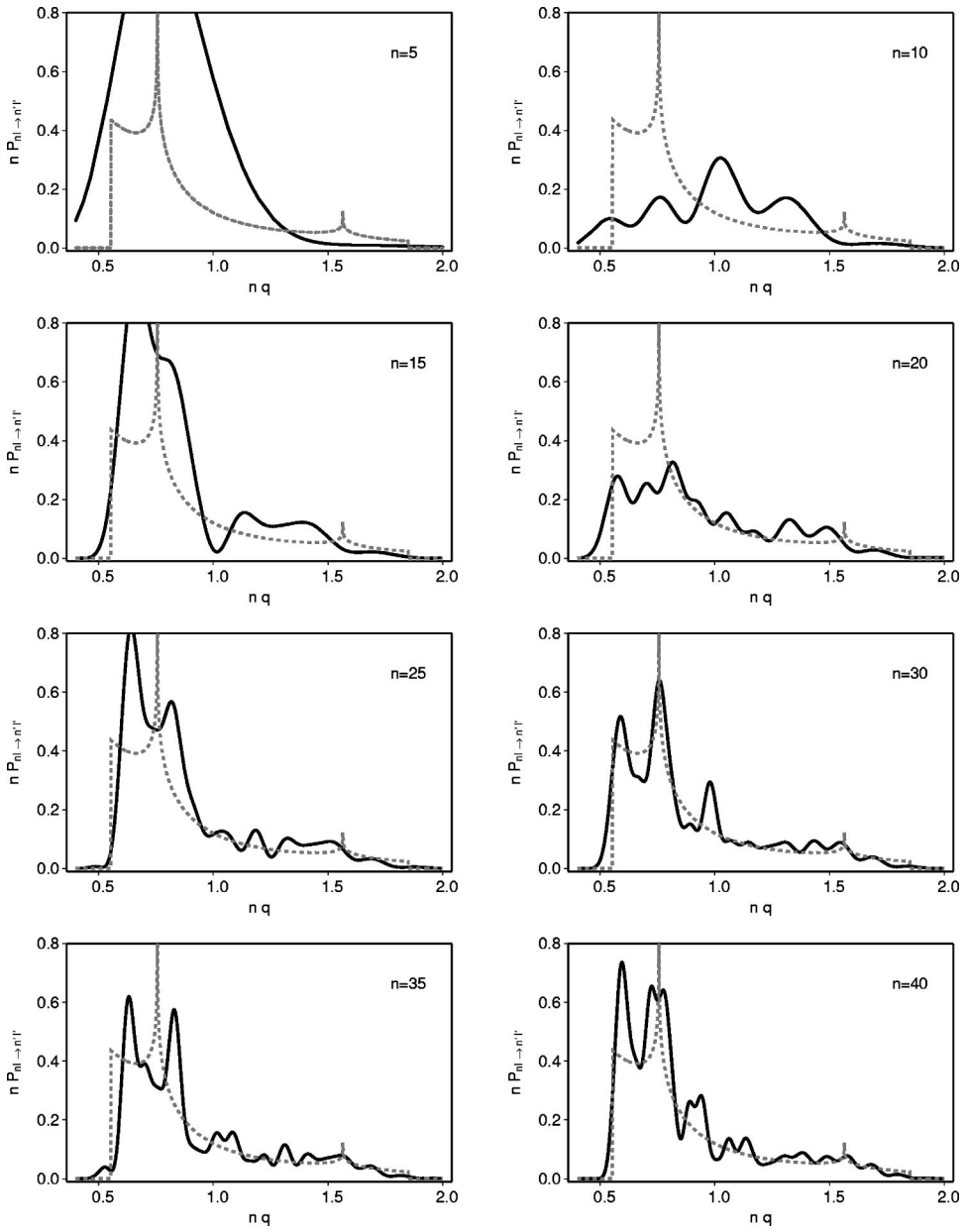

FIG. 6. Classical (dotted line) and quantal (solid line) symmetric scaled form factors as a function of scaled momentum transfer $\overline{q}=nq$ for $nl\rightarrow n'l'$ transitions. For fixed parameters $l/n=1/5$, $n'/n=7/5$, and $l'/n=6/5$, convergence is obtained as n is increased from $n=5$ to $n=40$.

angular momenta l and l'. The resulting angular momentum L is given by $L=|l-l'|+2s$, such that L takes values between $|l-l'|$ and $l+l'$ with the same parity as $l+l'$. The hypergeometric function ${}_2F_1$ reduces to a polynomial that obeys a simple recursion relation since either the first or the second argument of ${}_2F_1$ is a negative integer. The quantal form factor has, therefore, a very simple structure as a function of momentum transfer q, being a polynomial divided by $(1+q^2/\alpha^2)^{n+n'}$. Unfortunately, factorials of large arguments lead to very large but integer coefficients in the polynomial expression. Accurate results for $n>40$ cannot be obtained by using the usual floating-point machine accuracy. By using integer and rational number arithmetic, calculation can, however, be performed in infinite precision if the momentum transfer is approximated by a rational number. The result, in turn, is obtained as an exact rational number, with an extremely large numerator and denominator. Even though the form factor can be calculated in this way for arbitrary quantum numbers (computer time and memory being the only constraints), the results exhibit an increasing number of oscillations, as seen in $n>80$ subplots of Fig. 5. The usefulness of the exact, rigorous, quantal results, therefore, becomes questionable for such large quantum numbers and only an averaging procedure can provide practical quantitative results. The classical form factor has the ability to operate as an effective averaged version of the exact quantal counterpart, as illustrated in Fig. 5.

V. QUANTAL-CLASSICAL CONVERGENCE

Quantal-classical correspondence is evident when the classical curve provides the essential framework on which the quantal oscillatory structure is superimposed. In this sense, Fig. 5 illustrates the convergence of the scaled quantal

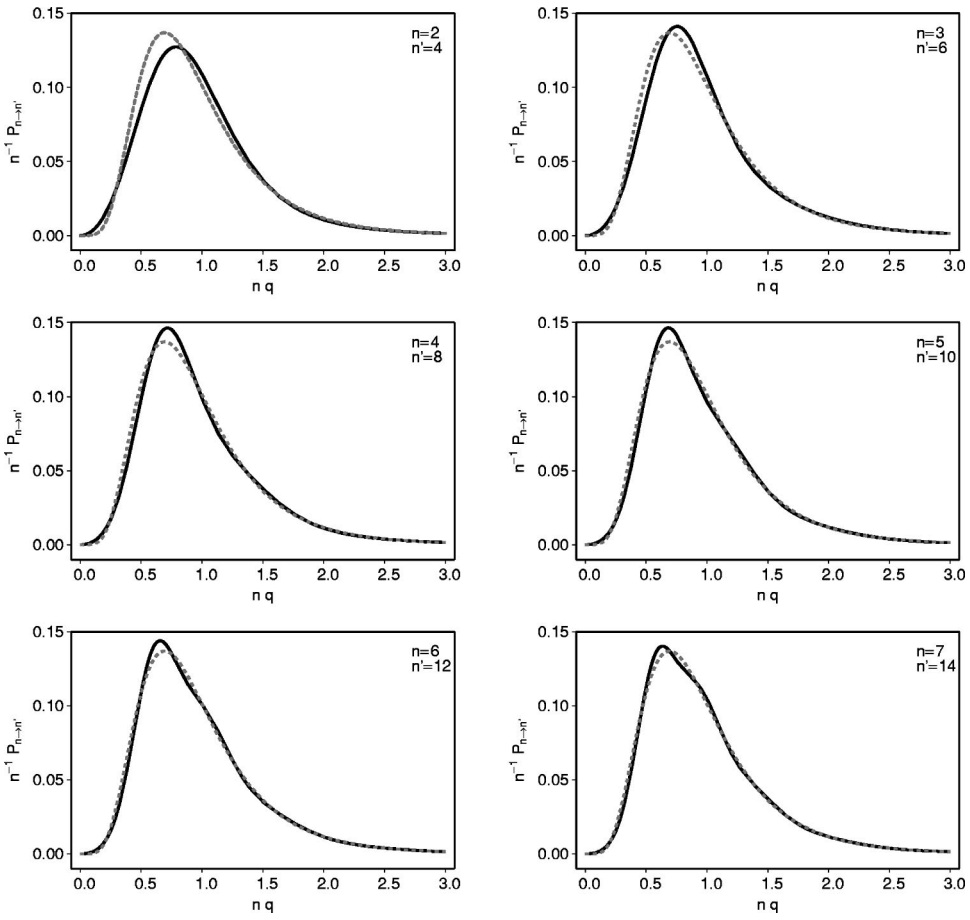

FIG. 7. Classical (dotted line) and quantal (solid line) scaled form factors as a function of scaled momentum transfer $\overline{q}=nq$ for $n\rightarrow n'$ transitions. For transitions with constant ratio $n'/n=2$, convergence is obtained as n increases from $n=2$ to $n=7$.

form factors $n^2P^Q_{nlm\rightarrow n'l'm}(\mathbf{q}/n)$ onto the universal classical curve $P^C_{1,l/n,m/n\rightarrow n'/n,l'/n,m/n}$ as a function of scaled q for $nlm\rightarrow n'l'm$ transitions. Convergence ranges from good for n as low as 30 to excellent for $n\geqslant 80$. The oscillations can be attributed to interference effects between phases (quantal or semiclassical) of the contributions to the amplitude that arises from each location r_k.

Convergence to the classical results is much faster when the results are averaged over all m values, as for the scaled probabilities $nP_{nl\rightarrow n'l'}$ for $nlm\rightarrow n'l'm$ transitions, displayed in Fig. 6. Finally, in Fig. 7, the classical and quantal probabilities $n^{-1}P_{n\rightarrow n'}$ for the l,m-averaged transitions contain no oscillatory structure and agree for n as low as 2. This result is well known and is the basis for classical descriptions of $n\rightarrow n'$ collisional transitions.

VI. CONCLUSION

Using the PSD formulation [13], the classical-quantal correspondence has been established by showing that the atomic form factor (1) for state-to-state transitions in a general one-electron atom can be written in the generic form (2) where the quantal and classical distributions are given by Eqs. (3) and (7), respectively. Exact calculations of the derived probability (50) for $nlm\rightarrow n'l'm$ transitions are presented. The classical state-to-state form factor (50) is expressed analytically in terms of the radial electronic locations r_k where the transitions occur. Agreement with previously published results [17] is obtained for the special case of atomic hydrogen (Coulombic potential).

The classical background contains two classical inaccessible regions (at small and large momentum transfers q) and four singularities attributed to four cases where two roots r_k converge for four values of q. The method also permits the construction of important classical scaling laws obeyed by the form factor for any $i\rightarrow f$ transition, involving bound or continuum states. Use of these scaling rules then facilitates a detailed investigation of the rate of convergence of the quantal results to the classical background, as n is increased. The quantal results at high n are shown to reduce to oscillatory structure superimposed on the classical background, as in Fig. 5. The rate of this convergence is accelerated upon averaging, in succession, over the m substates and then the l states, as for the $nl\rightarrow n'l'$ and $n\rightarrow n'$ transitions displayed in Figs. 6 and 7, respectively. Figures 5–7 also illustrate that classical form factors have the capability to operate as an effective and reliable averaged version of its quantal counterpart. This is of particular significance to experiments that involve very high values of $n\simeq 400$, as in the half-cycle experiments of Bromage and Stroud [4].

In summary, the phase-space distribution method [13] has permitted (a) universal scaling laws for the classical form factor to be immediately derived in transparent form, (b) the construction of an analytic expression (50) for the form factor for state-to-state transitions in a system with general interaction $V(r)$, and (c) the detailed numerical investigation

of the convergence of the quantal form factors onto the classical background.

ACKNOWLEDGMENTS

This work has been supported by AFOSR Grant No. 49620-99-1-0277 and NSF Grant No. 01-00890.

APPENDIX: COMPONENT OF ANGULAR MOMENTUM ALONG $\hat{\mathbf{q}}$

When the axis $\hat{\mathbf{z}}$ of atomic quantization is along the direction $\hat{\mathbf{q}}$ of the impulse, then

$$(\mathbf{r}\times\mathbf{p})\cdot\hat{\mathbf{z}}\equiv\frac{\mathbf{r}}{q}\cdot[\mathbf{p}\times(\mathbf{p}+\mathbf{q})]=\left[\frac{rp}{q}|\mathbf{p}+\mathbf{q}|\right]\sin\theta_{if}\cos\theta,$$

where the angles θ_{if} and θ are depicted in Fig. 3.

From the spherical triangles ABC and ABD, then

$$\frac{\sin V_i}{\sin U_f}=\frac{\sin V_f}{\sin U_i}=\frac{\sin A}{\sin\theta_{if}}$$

and

$$\cos\theta=\sin U_i\sin V_i,$$

respectively, so that

$$(\mathbf{r}\times\mathbf{p})\cdot\hat{\mathbf{z}}=\left[\frac{rp}{q}|\mathbf{p}+\mathbf{q}|\right]\sin U_i\sin U_f\sin A.$$

Since $\sin U_i=L_i/rp$ and $\sin U_f=L_f/r|\mathbf{p}+\mathbf{q}|$, then

$$(\mathbf{r}\times\mathbf{p})\cdot\hat{\mathbf{z}}=\left(\frac{L_iL_f}{qr}\right)\sin A,$$

as in Eq. (48) of the text. From spherical triangle ABC, the angle A is determined from

$$\cos A=\frac{\cos\theta_{if}-\cos U_i\cos U_f}{\sin U_i\sin U_f},$$

where

$$\cos\theta_{if}=\frac{p^2+|\mathbf{p}+\mathbf{q}|^2-q^2}{2p|\mathbf{p}+\mathbf{q}|}.$$

Since $p\cos u_i=\mu\dot{r}_i$ and $|\mathbf{p}+\mathbf{q}|\cos u_f=\mu\dot{r}_f$ in terms of the radial speeds, then A is determined from

$$\cos A_\pm=\left(\frac{r^2}{2L_iL_f}\right)[p^2+|\mathbf{p}+\mathbf{q}|^2\pm2\mu^2\dot{r}_i\dot{r}_f].$$

Under the constraints (41) and (42), then

$$\cos A_\pm=\frac{r^2}{2L_iL_f}C_\pm(r),$$

where

$$\begin{aligned}C_\pm(r)&=2\mu[E_i+E_f-2V(r)]\pm2\mu^2\dot{r}_i\dot{r}_f-q^2\\&=2\mu[E_i+E_f-2V(r)]\pm4\mu\left[E_i-V(r)-\frac{L_i^2}{r^2}\right]^{1/2}\\&\quad\times\left[E_f-V(r)-\frac{L_f^2}{r^2}\right]^{1/2}-q^2,\end{aligned}$$

as in Eq. (46) of the text.

[1] D. Vrinceanu and M. R. Flannery, Phys. Rev. Lett. **82**, 3412 (1999).
[2] M. R. Flannery, Phys. Rev. A **22**, 2408 (1980).
[3] C. O. Reinhold, J. Burgdörfer, M. T. Frey, and F. B. Dunning, Phys. Rev. Lett. **79**, 5226 (1997).
[4] J. Bromage and C. R. Stroud, Phys. Rev. Lett. **83**, 4963 (1999).
[5] B. E. Tannian *et al.*, J. Phys. B **32**, L517 (1999).
[6] E. M. Spain *et al.*, J. Chem. Phys. **102**, 9522 (1995).
[7] E. M. Spain *et al.*, J. Chem. Phys. **102**, 9532 (1995).
[8] W. A. Isaacs and M. A. Morrison, Phys. Rev. A **57**, R9 (1998).
[9] M. A. Morrison, E. G. Layton, and G. A. Parker, Phys. Rev. Lett. **84**, 1415 (2000).
[10] N. E. Shafer-Ray, M. A. Morrison, and G. A. Parker, J. Chem. Phys. **113**, 4274 (2000).
[11] S. K. Dutta *et al.*, Phys. Rev. Lett. **86**, 3993 (2001).
[12] M. R. Flannery and D. Vrinceanu, Phys. Rev. Lett. **85**, 1 (2000).
[13] D. Vrinceanu and M. R. Flannery, Phys. Rev. A **60**, 1053 (1999).
[14] I. Bersons and A. Kulsh, Phys. Rev. A **55**, 1674 (1997).
[15] K. Omidvar, Phys. Rev. **188**, 140 (1969).
[16] A. O. Barut and H. Kleinert, Phys. Rev. **160**, 1149 (1967).
[17] I. Bersons, A. Kulsh, and R. Veilande, Phys. Lett. A **277**, 223 (2000).
[18] D. Vrinceanu and M. R. Flannery, Phys. Rev. A **63**, 032701 (2001).